Simulation of the DVCS calorimeter with the GEANT4 toolkit

T. Zerguerras

▶ **To cite this version:**

T. Zerguerras. Simulation of the DVCS calorimeter with the GEANT4 toolkit. 2003, pp.32. in2p3-00012813

HAL Id: in2p3-00012813
https://hal.in2p3.fr/in2p3-00012813

Submitted on 26 May 2003

HAL is a multi-disciplinary open access archive for the deposit and dissemination of scientific research documents, whether they are published or not. The documents may come from teaching and research institutions in France or abroad, or from public or private research centers.

L'archive ouverte pluridisciplinaire **HAL**, est destinée au dépôt et à la diffusion de documents scientifiques de niveau recherche, publiés ou non, émanant des établissements d'enseignement et de recherche français ou étrangers, des laboratoires publics ou privés.

IPNO-03-04

Simulation of the DVCS calorimeter with the GEANT4 toolkit

Thomas ZERGUERRAS
RDD

Simulation of the DVCS calorimeter with the GEANT4 toolkit

T. Zerguerras
IPN Orsay

May 23, 2003

Abstract

This report presents a study of the calorimeter design for the Deep Virtual Compton Scattering experiment at CLAS (Jefferson Laboratory) using the GEANT4 simulation toolkit. The aim of this work is to evaluate the influence of the introduction of thin carbon cells around the $PbWO_4$ crystals of the calorimeter on the quality of the energy measurement. The methods used to construct the detector geometry, the physical processes and the primary event generator chosen with GEANT4 are described. Comparative results on the fraction of energy measured and on its energy resolution are presented.

1 Introduction

The DVCS (Deep Virtual Compton Scattering) experiment will be performed at the CEBAF accelerator at Jefferson Laboratory (Newport News, Virginia, USA) using a 6 GeV polarized electron beam, on a liquid hydrogen target. The $ep \rightarrow e'p\gamma$ reaction is produced by two different mechanisms: the Deep Virtual Compton Scattering (or DVCS) on the proton and the Bethe-Heitler process, this latter one being dominant by about two orders of magnitude. In most of the kinematical domain, there is an interference of these two processes which give rise to a beam spin asymetry $\mathcal{A}$ proportionnal to the DVCS process. To perform this experiment all the reaction products, including the photon, whose energy range is between 0.4 and 5.6GeV, must be detected. Theoretically, the DVCS process allows to access the Generalized Parton Distribution of the proton which provides information about the correlations between quarks inside the nucleon. Experimentally, the main difficulties come from the low counting rate for this reaction and the high background induced by the $ep \rightarrow e'p\pi^0$ reaction.

The detector which interests us here is the electromagnetic calorimeter, used for the detection of the final photon, produced during the DVCS process and mostly emitted in the forward direction. It will complete the standard CLAS (CEBAF Large Acceptance Spectrometer) detection system [1], composed of drift chambers, plastic scintillators, Cerenkov detectors, and large angles calorimeters. It will cover angles between 3° and 13° and will improve the photon detection efficiency and suppress the background contribution.

The construction of this calorimeter requires an important research and development work to determine the shape, size and material of the crystals to be used, as well as the mechanical set-up and the reading electronics. For the crystal, lead tungstanate ($PbWO_4$) is chosen because of its high density, fast response and good radiation hardness. As a trapping magnet is applied around the target, photomultipliers cannot be considered and avalanche photodiodes (APDs) are used to convert the scintillation light into electric signals. A temperature stabilization system must complete this set-up because the crystal and APD responses depend strongly on the temperature.

The geometry of the detector set-up influences the quality of the energy measurement. Two methods to assembly the crystals are proposed: either to pile up directly the crystals or to place them in alveols, like in the CMS experiment [2], in order to have a better mechanical stiffness. In the case of the DVCS calorimeter, the material proposed for theses alveols is carbon. Simulations with the GEANT4v4.1 toolkit are performed in order to check the influence of these alveols on the quality of energy measurement, in comparison with other limiting factors such as electronics noise and associated thresholds, and also to the pile-up structure without using such alveols.

2 Simulation programming

GEANT4 is a C++ written software which uses object oriented programming. The users implement their own classes derived from predefined abstract classes. Here we just give an overview of the main classes implemented in our study. The following is extracted from the GEANT4 Physics Reference Manual, full details are available in [3]:

- The user must construct a concrete class from the abstract `G4VUserDetectorConstruction` class to define the detector geometry. It also uses several pre-defined classes and associated methods to define geometrical shape, materials and place the created solids.
- A concrete class, derived from the abstract `G4VUserPhysicsList` class and its methods `ConstructParticle()` (construction of particles), `ConstructProcess()` (construction of processes) and `SetCuts()` (set of a cut range value for each particle) is also necessary for the physics part of the simulation. Predefined GEANT4 classes such as the `G4ParticleDefinition` class which allows to characterize the particles are also needed.
- The specification on the generation of the primary event (nature, energy, momentum direction, starting point of the particle) needs the implementation of a concrete class derived from the abstract `G4VUserPrimaryGeneratorAction` class. It consists in defining an instance of the `G4ParticleGun` class by setting primary particle parameters.
- Two other concrete classes are implemented to define the sensitive part of the detector and memorize the energy loss at each step. This makes the construction of histograms possible.

In the `main()` program, the user creates an instance of the `G4RunManager` class which controls the flow of the program, manages the initialization procedures and the event loop(s) within a run.

2.1 Geometry

Each $PbWO_4$ crystal of the calorimeter has the same trapezoidal shape (see fig. 1), with dimensions of $13.3\times13.3\text{mm}^2$ on the front face $16\times16\text{mm}^2$ on the back face, and is 160mm long, corresponding to 18 radiation lengths. These crystals are produced at the Bogoroditsk Technico-Chemical plant in Russia.

In the simulation program, four trapezoids of different materials are used to form an elementary cell: $PbWO_4$ crystal, air, aluminium envelop,

and carbon. The four trapezoids are then placed inside each other, beginning with the carbon and ending by the inner $PbWO_4$ (see fig. 1). The air and aluminium thicknesses are both 0.03 mm, carbon thickness is 0.15 mm so that the distance between two consecutive crystals is 0.42 mm ($2\times(0.15+0.03+0.03)$mm).

The whole calorimeter, shown on figure 2, is comprised of 424 cells. A central square hole, corresponding to 16 cells, is left free for the beam passage. This calorimeter covers angles between 3° and 13°. It is built around a focal point located at 800 mm from the detector. The target is placed at 650 mm from the detector. A succession of transformations including rotations around the X and Y axes and translations along the same axes are performed to place each cell at the right place. Rotation angles are multiples of 0.478°. In our study, we have to consider only a 5×5 matrix of cells because a shower mainly spreads on the closest neighbours of the hit crystal. As it is impossible to fill a spherical surface with squares, it is necessary to add a clearance of a few micrometers on the translation length to avoid overlapping between the cells. The translation length used in this case is 15.119mm if carbon alveols are included and 14.818 mm without them.

2.2 Physics Processes

Only electromagnetic processes are considered during this study and particles are either electrons, positrons or photons. Quantitative methods used by GEANT4 to compute physical processes are described in details in appendix A. Here only a qualitative summary of the physical processes which take place during the formation of the electromagnetic shower is given.

2.2.1 Photons

In the energy range considered here (a few GeV), the photon can interact with matter according to three processes [4]:

1. **Photoelectric effect:** This process involves the absorption of a photon by an atomic electron followed by the ejection of the electron from the atom.

2. **Compton Scattering:** The photon scatters on bound electrons, which can be considered as free if the photon energy is sufficiently high compared to the electron binding energy.

3. **Gamma conversion into an (e^+, e^-) pair:** The photon transforms into an electron-positron pair. This process is possible under two conditions:

   - to conserve momentum, a third body, usually a nucleus, is present.
   - the photon must have at least an energy of 1.022MeV.

This last process is dominant at high energy above a few GeV. It contributes mainly to the formation of a shower by producing new charged particles, which can in turn lose their energy by emitting energetic Bremsstrahlung photons (see section 2.2.2). The first two processes mentionned contribute mainly lower energy photons.

2.2.2 Electrons and positrons

Both electrons and positrons can interact through [4]:

1. **Multiple Scattering:** Charged particles suffer repeatedly elastic Coulomb scatterings from nuclei.

2. **Ionisation:** Like all charged particles, electrons and positrons suffer an energy loss in matter due to inelastic collisions with the atomic electrons of the material. The energy transfered to the atom could result in its ionisation.

3. **Bremsstrahlung:** Electrons and positrons are the only charged particles for which radiation contributes substantially to the energy loss of the particle. The Bremsstrahlung cross section varies as the inverse square of the particle mass and as the square of the atomic number of the material. This process contributes also to the development of the shower, creating photons which can in turn produce electron-positron pairs if they have sufficient energy (see in section 2.2.1).

A particular process for the positron should be added: **the e^+e^- Annihilation**. The positron annihilates with an electron of the absorber material to produce two photons. GEANT4 distinguishes between the "in flight" and "at rest" annihilation. This process occurs mainly for low energy or at rest positrons.

2.3 Energy cuts in GEANT4

In GEANT4, particles are tracked down to zero range/kinetic energy. Each particle has a threshold below which secondary particles will not be produced (production cuts). This threshold is a distance, or range, which is converted to an energy for all materials. These production cuts are needed because electromagnetic processes like Bremsstrahlung or δ ray productions involve infrared divergences. This can lead to the production of a large number of lower and lower energy photons or electrons. The production cuts limit this effect to particles above the threshold, the remainder being treated as a continuous effect.

An important feature in GEANT4 is the idea of an "unique cut value". It is used to handle cut values in a coherent manner. In this simulation, we have used the default cut-off value of 1mm for each particle in each material.

The corresponding energy values in each material used are shown in Table 1.

	Photon	Electron
Air	990eV	990eV
$PbWO_4$	84.8keV	1.13MeV
Carbon	3.29keV	568keV
Aluminium	6.89keV	597keV

Table 1: Energy cut-off values for different materials corresponding to the same range value of 1mm.

2.4 Primary Event Generator

To simulate the reactions inside the detector with GEANT4, it is necessary to define the initial conditions, including the nature of the particle generated, its energy, its momentum direction and its starting point position relative to the main frame (`World` volume).

In the present case, the primary event consists of the emission of an electron with a given energy, momentum direction, and starting point. The momentum direction is defined by two planar angles θ_{xz} in the xz plane and θ_{yz} in the yz plane (the z axis being the beam axis).

2.5 Creation of histograms in the Sensitive Detector

The total energy loss in the calorimeter and the associated resolution σ will be studied. We want to determine how these quantities vary for different momentum direction values. The electron can hit either in an active $PbWO_4$ crystal or in the dead zone of the calorimeter (air, aluminium or carbon).

To plot measured energy spectra, it is necessary to define the active part of the calorimeter, so that GEANT4 stores the useful informations, such as the ID number of each $PbWO_4$ and the individual energy measured in each of them. We will then deduce the total energy for each event by summing up the contributions of all crystals.

A total energy spectrum taking the noise and threshold effects of the reading electronics into account is also implemented. For each crystal, we add a random energy according a gaussian distribution with a σ of 15MeV and put an energy threshold of 30MeV. If the energy loss is below 30MeV (including the noise effect), the energy is put to 0. Then all crystals are summed up.

2.6 Validation test

The figures 3 and 4 show different views of a shower (one event) obtained with a 5×5 matrix, including the carbon alveols. It allows to check the geometry of the detector.

A validation test is then performed by generating 1000 events starting from the focal point located at 800mm from the detector. The bottom left corner coincides with the beam axis (z axis). The primary particle is a 2GeV electron and its momentum direction characterized by the two angle values $\theta_{xz} = \theta_{yz} = 2.5°$, such that the primary particle hits the matrix on the center of the central $PbWO_4$ crystal.

Figures 5 and 6 show respectively the energy spectra measured for each crystal and the total energy spectrum obtained for 1000 events with a 2 GeV electron starting from the focal point and hitting the 5×5 matrix at the center of the central crystal. The spectrum obtained by taking account of the electronics noise and thresholds is shown on figure 7.

A gaussian fit was performed on both spectra of figure 6 and 7. Results are shown in table 2. It shows already the influence of the electronics and threshold effects:

- The total energy measured is diminished by 5%.
- The σ resolution is degraded by near a factor 3.

	Centroid (GeV)	σ (MeV)
Without electronics effects	1.87	26
With electronics effects	1.77	70

Table 2: Mean energy and resolution obtained for a 2 GeV incident electron (Gaussian fit)

3 Study of the influence of carbon alveols

In order to know the influence of the carbon alveols, we have performed a comparative study by using two different crystal wrapping and assembly: one with and an other without carbon alveols. In terms of simulation parameters(see figure 1), that leads to a separation distance between the crystals of 0.12mm with air and aluminium only or 0.42mm if carbon alveols are included.

For each crystal assembly, we set a 5×5 matrix at two positions as shown in figure 8. The square full line zone, which will be called zone 1 in the following, is further from the symmetry axes of the set-up than the square

dotted line zone, called zone 2, which includes a dead zone on the vertical symetry axis.

The starting point of the 2GeV primary electron is located at the target point, at 650mm from the detector. The momentum direction is given by the two angles θ_{xz} and θ_{yz} as defined in section 2.4. We started from the center of the central crystal of the matrix and we scanned in the horizontal direction to the center of the two closest neighbouring crystals, i.e θ_{xz}varies, θ_{yz} being constant to 5.3°. The central position in zone 1 and zone 2 corresponds to θ_{xz}=5.3° and 0^o respectively.

For each value of θ_{xz}, we generate 1000 events and construct the energy spectra described in section 2.5. Except in specific case (see section 3.2), a gaussian fit is performed in order to obtain the mean energy loss (centroid) in the calorimeter and the resolution σ. In the next sections, we present the results obtained for the zones 1 and 2, with and without carbon alveols.

3.1 Results in zone 1

Energy loss spectra with and without taking the electronics effects into account have roughly the same shape than those presented in section 2.5, so gaussian fits can always be performed.

Figures 9 and 10 present the variations of the total energy loss and of the resolution in the calorimeter, for the two types of crystals assembly. The influence of the threshold (30MeV) and electronic noise (gaussian distribution with σ=15MeV) is also considered.

For both crystals assemblies, the introduction of the electronics effects decreases the total energy measured by about 5% and increase the resolution by more than a factor 2 (from about 28 MeV to 70 MeV).

When including the carbon alveols, we observe a slight decrease of about 4% of the total energy measured and an increase of 20 MeV of the energy resolution σ, between θ_{xz}= 4.8° and 5.9°. These particular angles are the worst cases as the electron hits the calorimeter in a dead zone, corresponding to the carbon alveols. For other angle values, the energy loss in the calorimeter and the energy resolution are very similar.

3.2 Results in zone 2

In zone 2, the matrix includes the vertical symmetry axis of the calorimeter, corresponding to θ_{xz}=0°. Two types of spectra are obtained, depending on θ_{xz} values. Figures 11 and 12 present the energy spectra, with and without the electronics effects, for a 2 GeV electron hitting the center of the central crystal (θ_{xz}=0.5°). These spectra are very similar to those obtained with the test matrix (see section 2.6) and for the study in zone 1 (see section 3.1). Figures 13 and 14 are the energy spectra for a 2GeV electron hitting the detector on the dead zone located on the symetry axis (θ_{xz}=0°). The

main peak observed in the former spectra around 1.7-1.8 GeV disappears. The measured energy is equal to 0 or gives continuous values up to 1.8 GeV.

Let's define the efficiency as the ratio of events with an energy mesured greater than 1.5 GeV for a 2 GeV incident electron. This threshold corresponds to a cut down to 3.8σ from the mean value of the energy measured in the standard conditions including noise effects (E=1.77 GeV, σ=70 MeV). On figure 15, the evolution of this parameter versus the angle values, with and without carbon alveols, is shown. In this study, the energy spectra contain electronics. One can see that the effect of the symetry axis is present in both cases but more accentuated for the matrix with carbon alveols. The inefficiency can reach up to 90% and the angular spread of this inefficiency region is 0.08°, corresponding to a distance of 1 mm on the crystal front face. If we perform the same study on the following dead zone, i.e the one next to the symetry axis, the effect is negligible without carbon alveols: the efficiency is always higher than 90%. However with the carbon alveols, an important effect can still be observed: efficiency peak is lower than 90% on a distance of 1mm on the crystal front face.

Figures 16 and 17 summarize the results for the energy loss measured in the calorimeter and for the associated resolution. No fit was performed in the two dead zones corresponding to the two θ_{xz} angular ranges [-0.04°;0.04°] and [1.17°; 1.25°]. Around the symetry axis, the degradation of the measurement is present for both matrix structure. In the neighbouring dead zone, a similar effect occurs only in the matrix including the carbon alveols. This effect is mainly due to the width of the dead zone which is greater by more than a factor 3 when carbon alveols are included. Even the incident electron can pass through a distance up to 100 mm in the detector dead zone before reaching an active crystal.

4 Summary and conclusions

For the Deep Virtual Compton Scattering experimental project at CLAS (Jefferson Laboratory), a calorimeter for photons detection is needed to upgrade the existing experimental set-up.

Simulations with the GEANT4 toolkit were performed to investigate a possible structure using carbon alveols around the active $PbWO_4$ crystals. Results show than when particles hit crystals away from the detector symetry axis, there is no important difference on the quality of energy measurement between structures with and without alveols. However, when an incident particle hits the calorimeter in a dead zone close to the symetry axis, the energy measurement is degraded. In the case of a structure with carbon alveols, this effect remains, although attenuated, in the closest neighbouring dead zones.

The crystal assembly with carbon alveols has the inconvenience to contain

dead zones. When these zones are located on or close to symetry axis, the particle hitting it has a higher probability to pass through the detector without interacting. It leads either to a lack of efficiency, because the particle cannot interact with the active part of the calorimeter, or gives an energy measurement value which does not correspond to the real energy of the interacting particle. However, other aspects, favorable to carbon alveole structure such as the mechanical stiffness and crystals safety must be taken into account.

5 Acknowledgements

The author wants to thank M. Guidal and M. Garçon for fruitful discussions on physics, J. Pouthas and P. Rosier for their help to understand the calorimeter mechanical set-up and I. Hrivnacova for her technical support on GEANT4.

A Appendix: GEANT4 standard electromagnetic package

This appendix is an excerpt of [5] , where quantitative details on the methods used by GEANT4 to simulate the different physical processes are given. The photon and charged particles (electron and positron) processes are distinguished.

A.1 Photon

In the energy range considered in this study, a photon could interact following three different mechanisms:

1. **Photoelectric effect**: GEANT4 uses the Biggs parametrization [6] to calculate the cross section $\sigma(Z, E_\gamma)$, which is a function of the atomic number Z and of the photon energy E_γ. In a given material, the mean free path λ is then calculated by:

$$\lambda = \left(\sum_i n_{ati} \sigma(Z_i, E_\gamma) \right)^{-1} \tag{1}$$

   where n_{ati} is the number of atoms per volume of the *ith* element of the material.

   The binding energies of the shells depend on the atomic number Z of the material. In compound materials the i^{th} element is chosen randomly according to the probability:

$$Prob(Z_i, E_\gamma) = \frac{n_{ati}\sigma(Z_i, E_\gamma)}{\sum_i [n_{ati}\sigma_i(E_\gamma)]} \tag{2}$$

   A photoelectron is emitted only if $E_\gamma > B_{shell}(Z_i)$, where $B_{shell}(Z_i)$ is the binding energy of the shell in the *ith* element of the material. The photoelectron kinetic energy is then given by:

$$T = E_\gamma - B_{shell}(Z_i) \tag{3}$$

   The polar angle of the photoelectron is then sampled from the Sauter-Gavrila distribution [7].

   In this implementation, the relaxation of the atom is not simulated and counted as a local energy deposited.

2. **Compton scattering:** To simulate Compton scattering of a photon from an atomic electron, GEANT4 uses an empirical cross section formula which reproduces the cross section data down to 10keV:

$$\sigma(Z, E_\gamma) = \left[P_1(Z) \frac{\log(1+2X)}{X} + \frac{P_2(Z) + P_3(Z)X + P_4(Z)X^2}{1 + aX + bX^2 + cX^3} \right] \tag{4}$$

where:

Z is the atomic number of the medium

E_γ the photon energy

$X = E_\gamma / mc^2$

m the electron mass

$P_i(Z) = Z(d_i + e_i Z + f_i Z^2)$

The interaction probability comes from a fit of all the parameters was made over 511 data points chosen from the intervals $1 \leq Z \leq 100$ and E_γ between 10keV and 100GeV.

The mean free path is then calculated by a similar formula as (1).
The sampling of the final state uses the Klein Nishina quantum model which gives the following expression for the differential cross section per atom [8]:

$$\frac{d\sigma}{d\epsilon} = \pi r_e^2 \frac{m_e c^2}{E_0} Z \left[\frac{1}{\epsilon} + \epsilon\right] \left[1 - \frac{\epsilon \sin^2\theta}{1+\epsilon^2}\right] \tag{5}$$

where:

r_e is the classical electron radius

$m_e c^2$ the electron mass

E_0 the energy of the incident photon

E_1 the energy of the scattered photon

$\epsilon = E_1 / E_0$

After the determination of ϵ through a Monte-Carlo method apply to the distribution (5) and assuming that the collision is elastic, the scattering angle θ can be obtained from the well known Compton formula:

$$E_1 = E_0 \frac{m_e c^2}{m_e c^2 + E_0(1 - \cos\theta)} \tag{6}$$

The azimuthal angle ϕ is generated isotropically. The kinetic energy and momentum of the recoil electron are deduced from momentum and energy conservation:

$$\begin{aligned} T_{el} &= E_0 - E_1 \\ \overrightarrow{P_{el}} &= \overrightarrow{P_{\gamma 0}} - \overrightarrow{P_{\gamma 1}} \end{aligned}$$

3. **Gamma Conversion into an (e^+, e^-) Pair:** GEANT4 takes as the total cross section per atom for the conversion of a photon into an (e^+, e^-) pair the following parameterization:

$$\sigma(Z, E_\gamma) = Z(Z+1)\left[F_1(X) + F_2(X)Z + \frac{F_3(X)}{Z}\right] \tag{7}$$

where E_γ is the incident photon energy and $X = ln(E_\gamma/m_e c^2)$. The functions F_n are polynomial functions of the 5^{th} order in X. Their parameters are taken from a least squares fit to the data [9]. This parameterization describes the data in the range $1 \leq Z \leq 100$ and for E_γ between 1.5MeV and 100GeV.

The mean free path λ for a photon to convert into an (e^+, e^-) pair is given by a similar expression as (1). The differential cross section depends on the atomic number Z of the material in which the interaction occurs. In a compound material the probability for which the interaction occurs in the i^{th} element is given by the same expression than (2).

The sampling of the final state uses the corrected Bethe-Heitler formula [10] for the differential cross section to obtain the quantity $\epsilon = E/E_\gamma$, where E_γ is the energy of the photon and E the total energy carried by one particle of the (e^+, e^-) pair. The kinematical limits of ϵ are therefore:

$$\frac{m_e c^2}{E_\gamma} = \epsilon_0 \leq \epsilon \leq 1 - \epsilon_0 \tag{8}$$

Details for the generation process of ϵ could be find in [5]. Once this value is obtained, the charge of each particle of the pair is chosen randomly and the polar angle of the electron (or positron) is defined with respect to the direction of the parent photon. GEANT4 approximates the energy-angle distribution by the Urban density function [11] in order to obtain the polar angle from ϵ value. The azimuthal angle is generated isotropically. The final state is then completely determined according to the coplanarity of the e^+ and e^- momenta with the parent photon and to the energy conservation.

A.2 Electron and positron

1. **Multiple Scattering (MSC):** To simulate the multiple scattering of charged particles in matter, GEANT4 uses a model based on the Lewis theory [12]. The model simulates the scattering of the particle after a given step, computes the path length correction and the lateral displacement. It belongs to the class of condensed simulations, i.e. the global effect of the collisions is simulated after a track segment. These effects are the net displacement, energy loss and change of direction

of the charged particle. One of the advantage of the Lewis theory, compared to other models (Molière model [13], Goudsmit-Saunderson model [14]), is that it computes not only the angular distribution after a step, but also the moments of the spatial distribution. Model functions determine angular and spatial distributions after a step [5]. These functions have been chosen in such a way that they give the same moments of the (angular and spatial) distributions than the Lewis theory.

Two path lengths are used during the computation process:

- the true path length ('t' path length) is the total length travelled by the particle. All the physical processes restrict this 't' step.
- the geometrical (or 'z') path length is the straight distance between starting and end point of the step. The detector geometry limits the 'z' step.

The MSC algorithm compares these both steps and takes the minimum as the step length. Then it calculates the relocation of the particle and the new 't' path length to perform the following energy loss and scattering calculations.

The scattering angle θ of the particle after the step of length 't' is then sampled. The azimuthal angle ϕ is generated isotropically. After the simulation of the scattering, the lateral displacement is computed. It is also checked that the relocation of the particle with the lateral displacement does not take the particle beyond the volume boundary.

2. **Ionisation:** GEANT4 allows to calculate thecontinuous and discrete energy losses of electrons and positrons due toionization in a material. Above a given energy threshold, the energy loss is simulated by the explicit production of δ rays by Möller scattering (e^-e^-) or Bhabha scattering (e^-e^+). Below the threshold, the soft electrons ejected are simulated as a continuous energy loss of the incident $e^\pm$.

   Both for continuous energy loss and the δ ray energy spectrum, the method used consists in integrating the differential cross section per atom for the ejection of an electron $\frac{d\sigma(Z,E,T)}{dT}$. T is the kinetic energy of the ejected electron, E is the total energy of the incident $e^\pm$, and Z is the atomic number of the material. The mean rate of energy loss by the incident $e^\pm$ due to soft δ rays has the form:

$$\frac{dE_{soft}(E,T_{cut})}{dx} = n_{at}\int_{T_{cut}}^{T_{max}} \frac{d\sigma(Z,E,T)}{dT} dT \tag{9}$$

   where n_{at} is the number of atoms per volume in the material. T_{cut} is the energy below which δ rays are not explicitely produced, but treated as continuous energy loss. In GEANT4, T_{cut} is always 1keV or larger

and is referred as the *kinetic energy cut-off* or the *production threshold for δ rays*. For the ejection of an electron with an energy above T_{cut}, the total cross section per atom becomes:

$$\sigma(Z, E, T_{cut}) = \int_{Tcut}^{T_{max}} \frac{d\sigma(Z, E, T)}{dT} dT \tag{10}$$

where T_{max} is the maximum energy transferable to a free electron:

$$T_{max} = \begin{cases} E - mc^2 & \text{for } e^+ \\ (E - mc^2)/2 & \text{for } e^- \end{cases} \tag{11}$$

3. **Bremsstrahlung:** GEANT4 includes a numeric method to calculate the energy of electrons and positrons due to the radiation of photons in the field of a nucleus. Above a given threshold energy, the energy loss is simulated by the explicit production of photons. Below the threshold, the emission of soft photons is treated as a continuous energy loss. The formula used for this simulation are very similar to those used in GEANT3 [15]. However, in GEANT4, both the Landau-Pomeranchuk-Migdal effect and the dielectric suppression [16, 17] of the Bremsstrahlung have been implemented.

   The differential cross section for the production of a photon of energy k by an electron of kinetic energy T in the field of an atom of charge Z is noted $d\sigma(Z, T, k)/dk$. If k_c is the energy cutt-off below which the soft photons are treated as continuous energy loss, the mean value of the energy lost by the electron is:

$$E_{Loss}^{brem}(Z, T, k_c) = \int_0^{k_c} k \frac{d\sigma(Z, T, k)}{dk} dk \tag{12}$$

   The total cross section for the emission of a photon of energy larger than k_c is :

$$\sigma_{brem}(Z, T, k_c) = \int_{k_c}^{T} \frac{d\sigma(Z, T, k)}{dk} dk \tag{13}$$

   Many theories of the Bremsstrahlung process exist, with their own limitations and regions of applicability. A synthesis could be found in [18], where a tabulation of $d\sigma/dk$ for electrons with kinetic energies T from 1keV to 10GeV is also given. GEANT4 uses this tabulation, together with the corrected Bethe-Heitler formula at energies above 10GeV, including the dielectric suppression which also be applied to the Seltzer and Berger results in the calculation of the 'low energy' ($T \leq 10GeV$) data.

In the Bremsstrahlung process, the longitudinal momentum transfer from the nucleus to the electron can be very small. Thus, the uncertainty principle requires that the emission takes place over a comparatively long distance [19]:

$$f_v \sim \frac{2\hbar c\gamma^2}{k} \tag{14}$$

f_v is called the *formation length for Bremsstrahlung in the vacuum.* It is the distance required for the electron and photon to separate enough to be considered as separate particles. If anything happens to the electron or photon while traversing this distance, the emission can be disrupted. Two mechanisms, which are taken into account in GEANT4, could reduce this length:

- **The dielectric suppression** is due to the photon interaction with the electron gas (Compton scattering) within the formation length. As a consequence, the formation length in the considered medium, is reduced following:

$$f_m \sim \frac{2\hbar c\gamma^2 k}{k^2 + (\gamma\hbar\omega_p)^2} \tag{15}$$

  where ω_p is related to the dielectric function by:

$$\epsilon(k) = 1 - (\hbar\omega_p/k)^2 \tag{16}$$

  Moreover, the differential cross section is multiplied by a corrective factor, the suppression function:

$$S_d(k) \stackrel{def}{=} \frac{f_m(k)}{f_v(k)} = \frac{k^2}{k^2 + (\gamma\hbar\omega_p)^2} \tag{17}$$

- **The Landau-Pomeranchuk-Migdal suppression** is due to the multiple scattering of the electron with the atoms of the medium while it is still in the formation zone. If the angle of multiple scattering θ_{ms} is greater than the typical emission angle of the emitted photon $\theta_{br} = mc^2/E$, the emission is suppressed. That suppression becomes signifiant for photon energies below a certain value given by:

$$\frac{k}{E} < \frac{E}{E_{lpm}} \tag{18}$$

  E_{lpm} is a characteristic energy of the effect and could be parameterized following:

$$E_{lpm} \sim (7.7 \text{ TeV/cm}) \times X_0 \text{ (cm)} \tag{19}$$

where X_0 is the radiation length given by Tsai formula [20]. As for the dielectric suppression, this effect introduces the suppression function $S_{lmp}(k)$. If $f_m(k)$ is the formation length in the material, for $kE_{lpm} \ll E^2$:

$$S_{lpm}(k) \stackrel{def}{=} \frac{f_m(k)}{f_v(k)} = \sqrt{\frac{kE_{lpm}}{E^2}} \tag{20}$$

where:

$$f_m(k) \approx \frac{2\hbar c\gamma^2}{k}\sqrt{\frac{kE_{lpm}}{E^2}} \tag{21}$$

The total suppression, taking these two effects into account, follows [16]:

$$\frac{1}{S} = 1 + \frac{1}{S_d} + \frac{S}{S_{lpm}^2} \tag{22}$$

4. **e^+e^- Annihilation:** The cross section per atom for the annihilation in fly of e^+e^- into two photons is given by the Heitler formula [10, 21]:

$$\sigma(Z,E) = \frac{Z\pi r_e^2}{\gamma+1}\left[\frac{\gamma^2+4\gamma+1}{\gamma^2-1}\ln\left(\gamma+\sqrt{\gamma^2-1}\right) - \frac{\gamma+3}{\sqrt{\gamma^2-1}}\right] \tag{23}$$

with:

Z atomic number of the material

E total energy of the incident positron

$\gamma = E/mc^2$

m the electron mass

r_e classical electron radius

In a given material, the mean free path λ for a positron to be annihilated with an electron is given by:

$$\lambda(E) = \left(\sum_i n_{ati}.\sigma\left(Z_i,E\right)\right) \tag{24}$$

where n_{ati} is the number of atoms per volume of the i^th element composing the material.
According to the energy and momentum conservation the ratio of energy transfered to one of the two photons (designed by the subscript $_a$) is given by:

$$\epsilon = \frac{E_a}{E_{tot}} \equiv \frac{E_a}{T+2mc^2} \tag{25}$$

where E_{tot} is the total available enery and T the kinetic energy of the e^+. If Pc is the positron momentum, this ratio is in the range $[\epsilon_{min}, \epsilon_{max}]$ where:

$$\epsilon_{min} = \frac{E_{tot} - Pc}{2E_{tot}} \tag{26}$$

$$\epsilon_{max} = 1 - \epsilon_{min} \tag{27}$$

The maximum (resp. minimum) is obtained when the photon considered is emitted in the direction (resp. opposite direction) of the incident e^+.
The sampling of the photon energy follows the differential cross section of the two-photon e^+e^- annihilation [10, 21]:

$$\frac{d\sigma(Z,\epsilon)}{d\epsilon} = \frac{Z\pi r_e^2}{\gamma - 1}\frac{1}{\epsilon}\left[1 + \frac{2\gamma}{(\gamma+1)^2} - \epsilon - \frac{1}{(\gamma+1)^2}\frac{1}{\epsilon}\right] \tag{28}$$

ϵ is then generated following the distribution (28) and the photon energies are $E_a = \epsilon E_{tot}$ and $E_b = (1-\epsilon)E_{tot}$.

If θ is the angle between the incident e^+ and the photon γ_a, we have from energy-momentum conservation:

$$\cos\theta = \frac{1}{Pc}\left[T + mc^2\frac{2\epsilon - 1}{\epsilon}\right] \tag{29}$$

The azimuthal angle ϕ is generated isotropically. Thus the final state computation is complete.

GEANT4 also uses a specific method to treate the particular case arising when a positron comes at rest before annihilation. It generates two photons with energy mc^2, the angular distribution being isotropic.

References

[1] B.A. Mecking et al., Nucl. Inst. Meth. A503 (2003) 513.

[2] CERN/LHCC 97-33, CMS TDR 4, 15 December 1997.

[3] GEANT4 User's Guide, Version 4.1, June 2002.

[4] W.R. Leo, Techniques for Nuclear and Particle Physics Experiments, Second Revised Edition, Springer-Verlag (1994).

[5] GEANT4 Physics Reference Manual, June 25, 2002

[6] F. Biggs and R. Lighthill, PrePrint Sandia Laboratory, SAND87-0070 (1990).

[7] M. Gavrila, Phys. Rev. 113,514 (1959).

[8] O. Klein and Y. Nishina, Z. Physik 52 853 (1929).

[9] J.H. Hubbell, H.A. Gimm, I. Overbo, Jou. phys. Chem. Ref. Data 9:1023 (1980).

[10] W. Heitler, The Quantum Theory of Radiation, Oxford University Press (1957).

[11] L. Urban in GEANT3 writeup, section PHYS-211. Cern Program Library (1993).

[12] H.W. Lewis, Phys. Rev. 78 (1950) 526.

[13] Z. Naturforsch. 3a (1948) 78.

[14] S. Goudsmit and J.L. Saunderson, Phys. Rev. 57 (1940) 24.

[15] GEANT3 manual, CERN Program Library Long Writeup W5013 (October 1994).

[16] V.M. Galitsky and I.I Gurevich, Nuovo Cimento 32 (1964) 1820.

[17] P.L. Anthony et al., SLAC-PUB-7413/LBNL-40054 (February 1997).

[18] S.M. Seltzer and M.J. Berger, Nucl. Inst. Meth. 80 (1985) 12.

[19] M. Maire, Lecture at the GEANT4 Users Workshop, CERN, November 11^{th}-15^{th} 2002.

[20] Y.S. Tsai, Rev. Mod. Phys. 46, (1974) 815.
Y.S. Tsai, Rev. Mod. Phys. 49, (1977) 421.

[21] R. Ford and W. Nelson, SLAC-265, UC-32 (1985).

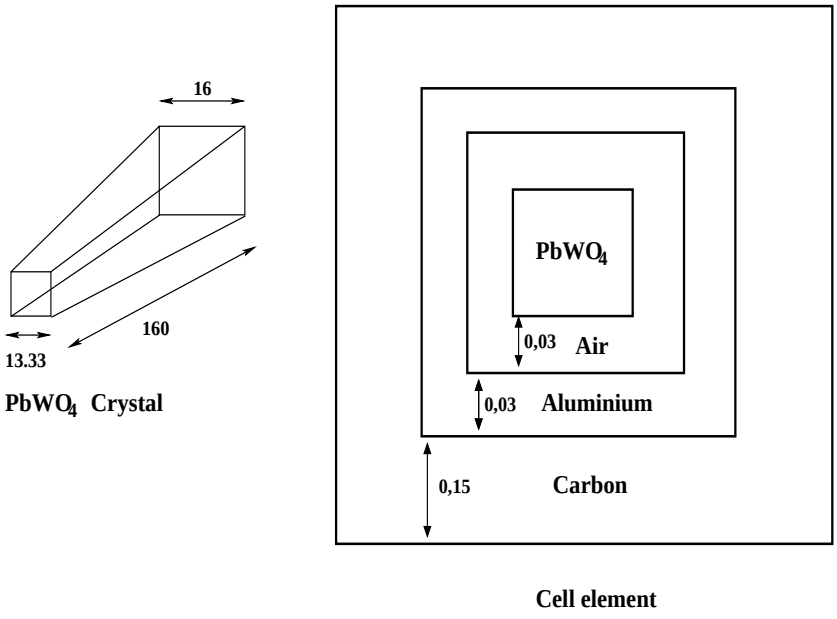

Figure 1: Geometrical shape of a $PbWO_4$ crystal (left) and the cell structure used in the simulation (right).

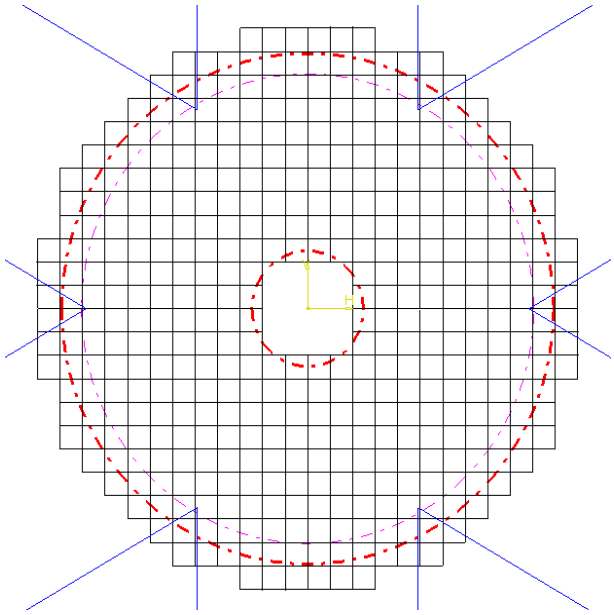

Figure 2: View of the front face of the calorimeter.

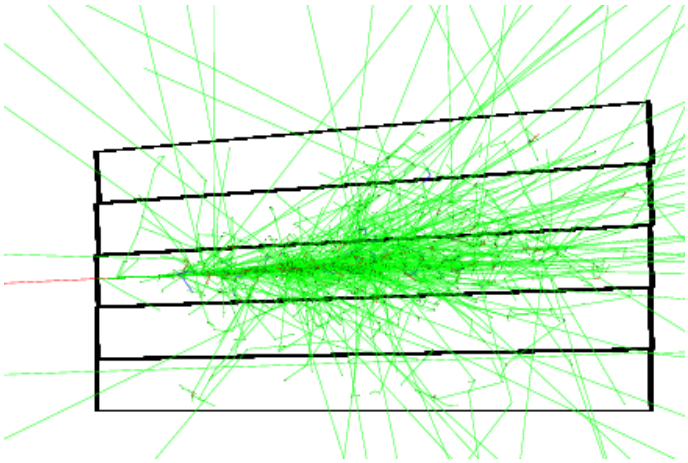

Figure 3: Upper view of a shower created by a 2 GeV electron in the center of a 5×5 matrix in the xz plane.

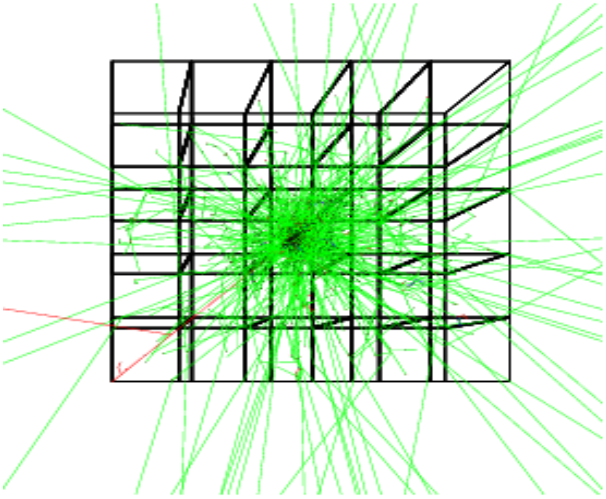

Figure 4: Front view of a shower created by a 2 GeV electron in the center of a 5×5 matrix in the xy plane.

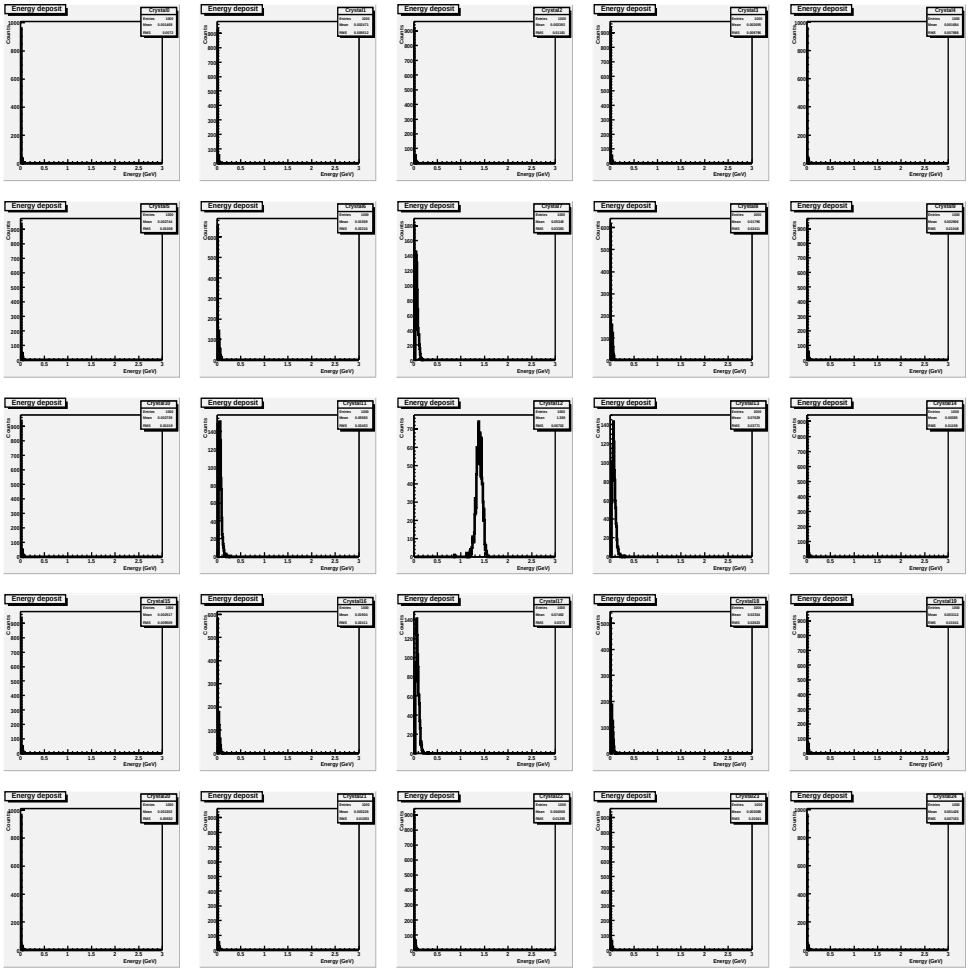

Figure 5: Histograms of the individual energy measured in each crystal of a 5×5 matrix for a 2 GeV incident electron on the center of the central crystal.

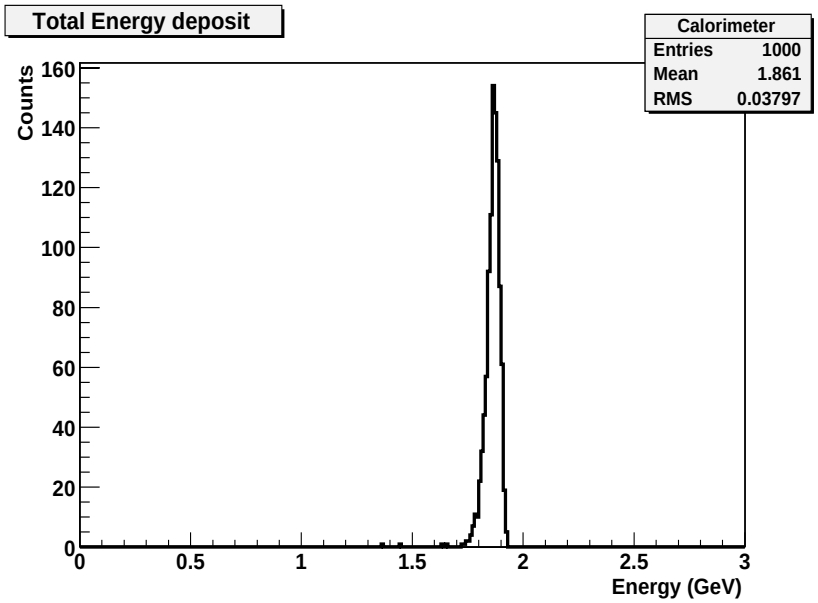

Figure 6: Total energy spectrum measured with a 2 GeV incident electron on the center of the central crystal of a 5×5 matrix.

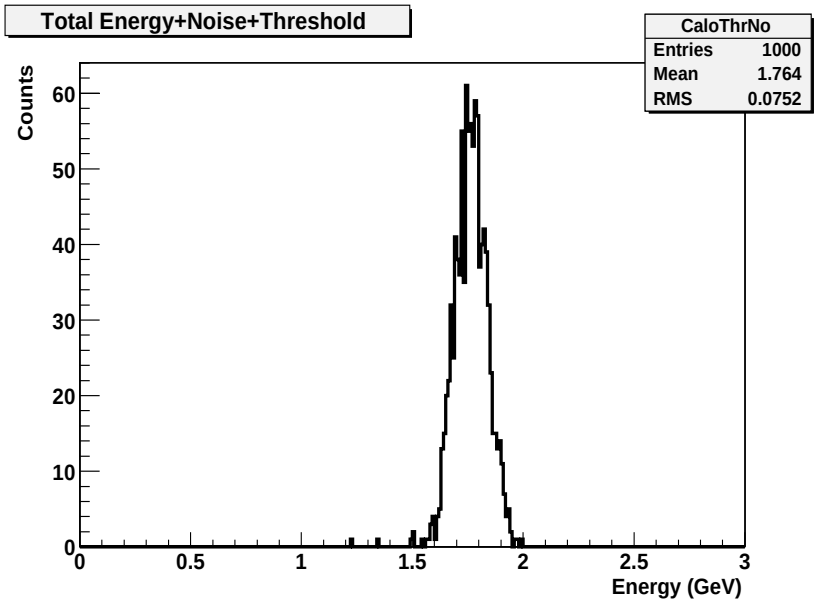

Figure 7: Total energy spectra measured with a 2 GeV incident electron on the center of the central crystal of a 5×5 matrix, including electronics noise and threshold effects.

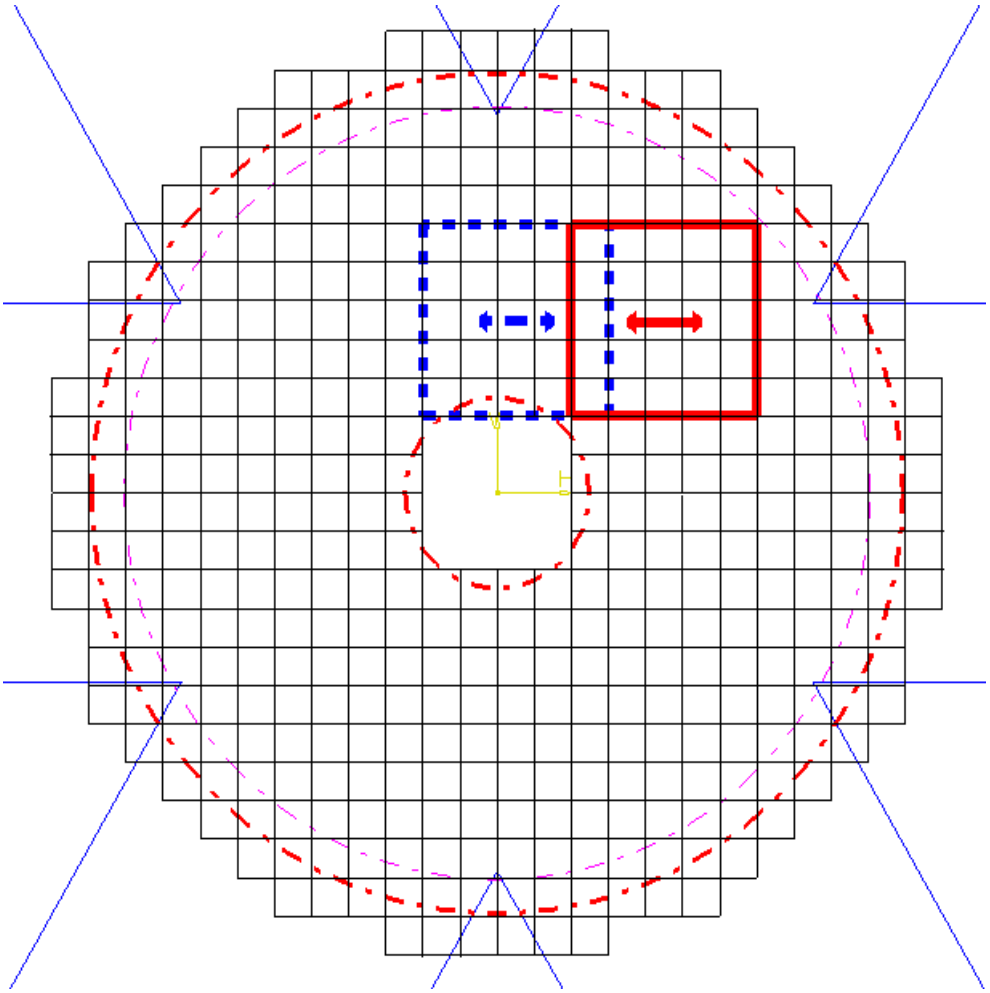

Figure 8: Geometrical position of the 5×5 matrix in zone 1 (square with thick full line) and 2 (square with thick dotted line). The double arrows indicate the scanning range for each case.

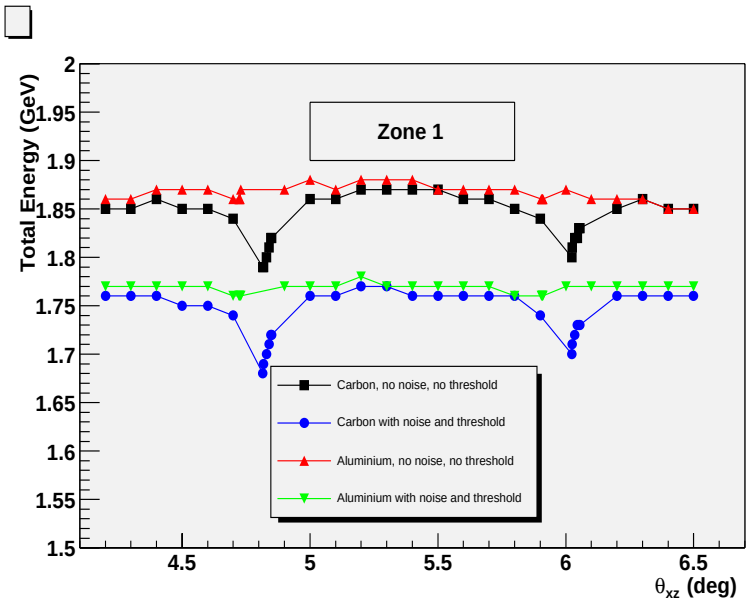

Figure 9: Evolution of the total energy loss in the calorimeter following θ_{xz} in zone 1.

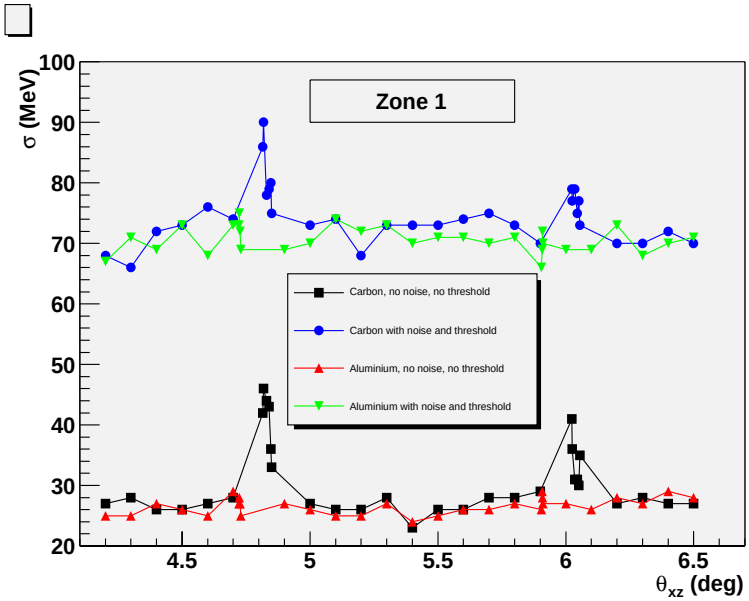

Figure 10: Evolution of the energy resolution of the calorimeter following θ_{xz} in zone 1.

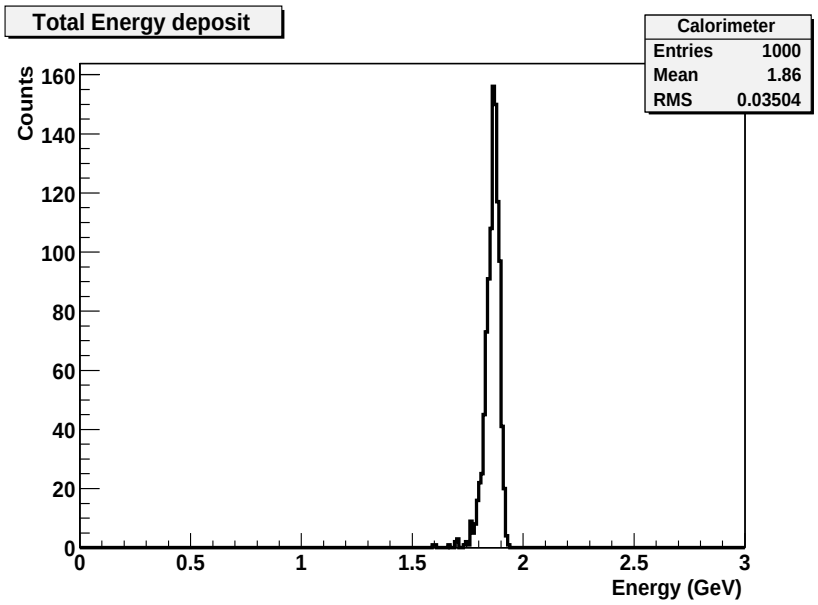

Figure 11: Total energy spectrum measured for a 2 GeV incident electron in the zone 2 with carbon alveols and θ_{xz}=0.5°, without taking the electronics effects into account .

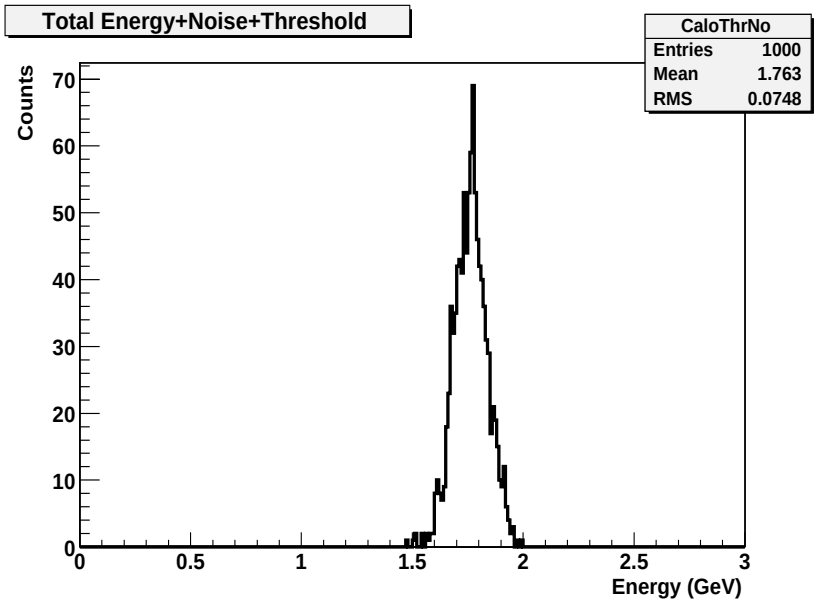

Figure 12: Total energy spectrum measured for a 2 GeV incident electron in zone 2 with carbon alveols, taking the electronic effects into account and θ_{xz}=0.5°.

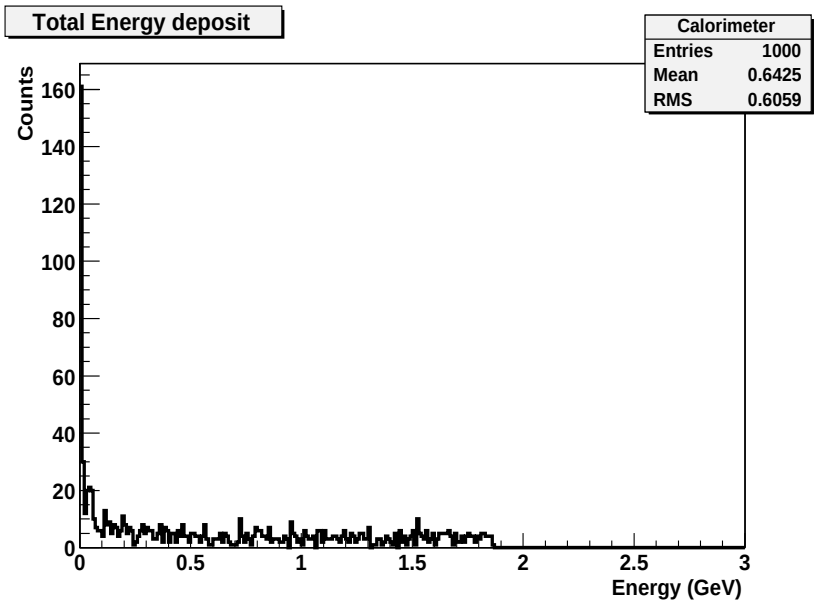

Figure 13: Total energy spectrum measured for a 2 GeV incident electron in zone 2 with carbon alveols and θ_{xz}=0°, without taking the electronic effects into account .

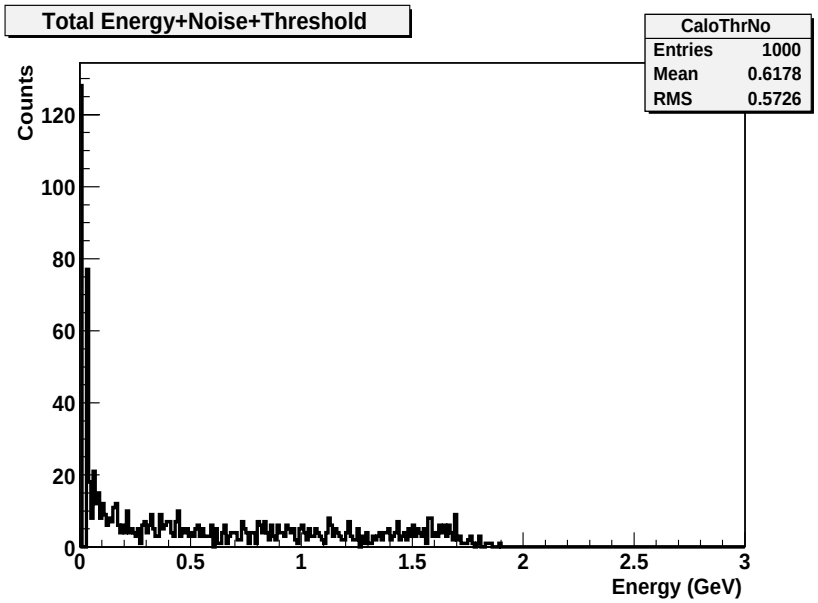

Figure 14: Total energy spectrum measured for a 2GeV incident electron in zone 2 with carbon alveols, taking the electronics effects into account and θ_{xz}=0°.

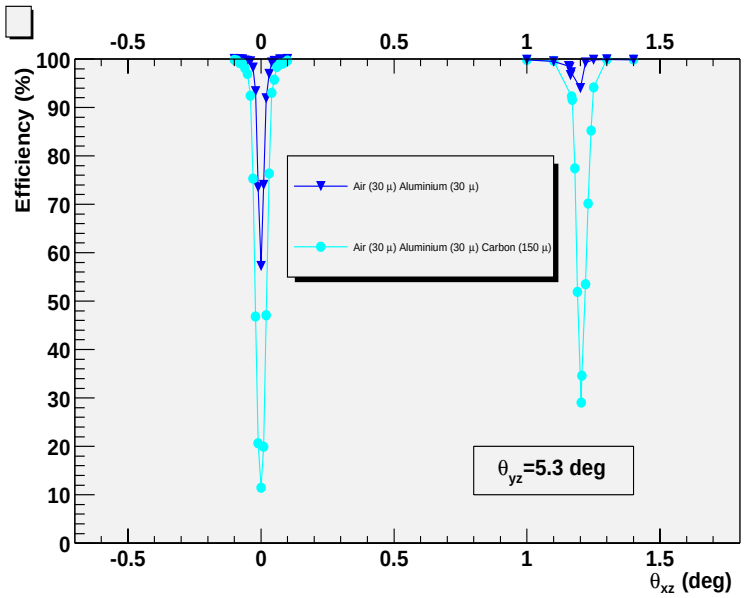

Figure 15: Efficiency following θ_{xz} in an area covering the symetry axis and one of the closest neighbouring dead zone.

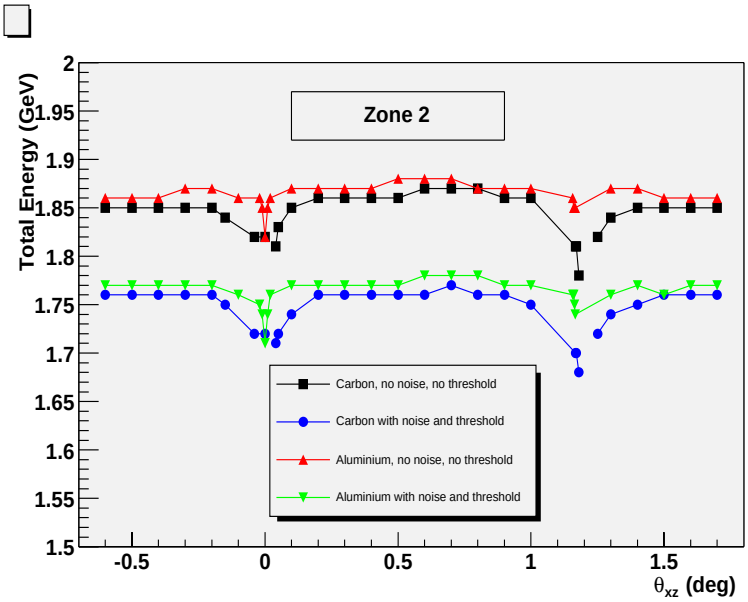

Figure 16: Evolution of the total energy loss in the calorimeter following θ_{xz} in zone 2.

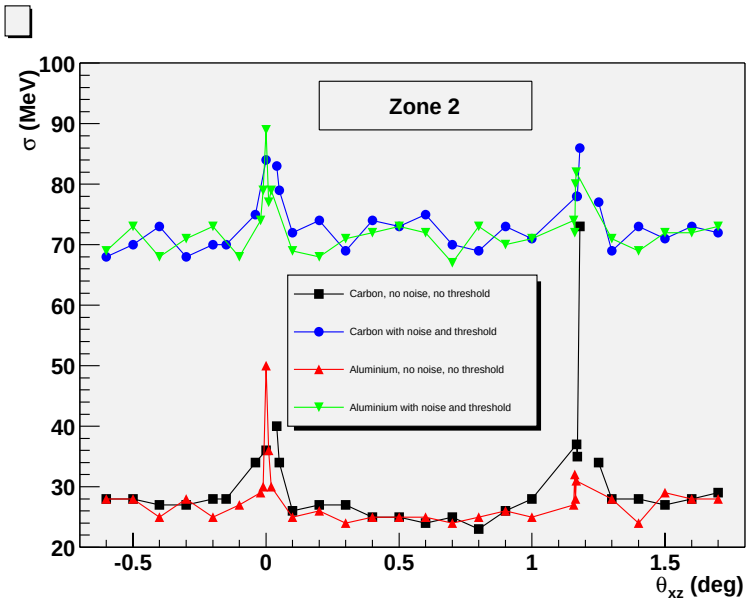

Figure 17: Evolution of the energy resolution of the calorimeter following θ_{xz} in zone 2.

List of Tables

List of Figures

Contents